https://ntrs.nasa.gov/search.jsp?R=19660023888 2018-07-25T00:33:25+00:00Z

N66 33178 (ACCESSION NUMBER) (THRU)
33 (PAGES) 1 (CODE)
CR-64059 (NASA CR OR TMX OR AD NUMBER) 23 (CATEGORY)
FACILITY FORM 602

GPO PRICE $
CFSTI PRICE(S) $
Hard copy (HC) 2.00
Microfiche (MF) .50
ff 653 July 65

On the use of Thermopiles for Absolute Radiometry in the Far Ultraviolet*

by

R.G. Johnston and R.P. Madden

National Bureau of Standards, Washington, D. C.

Abstract

Thermopiles used for absolute radiometry in the far ultraviolet spectral region are generally calibrated with visible and near-infrared radiation. Three possibilities for the failure of the sensitivity of thermopiles to be independent of wavelength have been investigated. It was found that gold-black typical of that used on thermopiles for far ultraviolet applications reflectively scattered 2 - 4% of the incident far ultraviolet radiation. Since the same gold black scattered a similar fraction incident visible and near-infrared radiation, the correction for this effect was small. An analysis of surface sensitivity maps indicated that a thermopile of 0.04 sec time constant showed no wavelength variation of sensitivity when either d.c. detection or a.c. synchronous detection with 13 c/s chopping was used. The most significant wavelength-dependent phenomenon of importance was found to be the photoelectric effect. Ejected electrons carry a significant amount of energy away from gold-blacked thermopiles in the spectral region below 1600Å. The maximum correction determined for a particular thermopile was 5.2% at 735Å.

[redacted]

*Work supported by the National Aeronautics and Space Administration

I. Introduction

Thermopiles have often been used in the vacuum ultraviolet spectral region as absolute detectors. Much of the data which exists on photoionization yields in gases[1-3] and photoelectric yields for solids[4-7,1] in the vacuum ultraviolet depends on thermal detection for the absolute measurement of radiant flux. Furthermore, the wavelength dependence of the efficiency of far ultraviolet radiation detectors is often determined by comparison to the fluorescent yield of a sodium salicylate phosphor, the relative response of which was determined by comparison with that of a thermopile.[8-10]

A thermopile destined for use as a standard in the vacuum ultraviolet is first calibrated in the visible region with sources of known blackness and temperature. It is then assumed that the thermopile will develop a given voltage for a specific wattage of incident radiant energy, independent of the wavelength of the radiation. This paper reports on the investigation of three possibilities for the failure of this assumption. First, the fraction of incident radiation reflectively scattered by the thermopile "black" has been measured in the visible and the far ultraviolet. Second, the energy carried away from the thermopile by photo-ejected electrons has been determined. Finally, the thermopile surface sensitivity has been mapped at several wavelengths using both a.c. and d.c. methods to reveal any wavelength dependence of the thermopile time constant.[11] Such a dependence would, of course,

[redacted]

influence the calibration of the thermopile if a.c. methods were employed.

The first possibility mentioned above, namely the failure of the "blackness" to be independent of wavelength, has been partially checked in a few instances. The specularly reflected component has been found small by several investigators,[12,13] but the determination of the total scattered radiation from such "blacks" has not been previously undertaken in the vacuum ultraviolet. The energy loss due to photo-ejected electrons had apparently been overlooked previous to the initiation of the present study, although it is well known that most surfaces exhibit a marked increase in photoelectric yield when the photon energy exceeds 9-10 eV.[6,1,7]

The present studies were conducted using a particular type of thermopile and black, however, the ones chosen are typical of those which have been used in the far ultraviolet as absolute detectors. Also, these results bear on the general problem of the applicability of thermal detectors for absolute radiometry in the far ultraviolet.

II. Reflective Scattering from Gold Black

A. Experimental Arrangement

1. Source and Monochromator

A normal-incidence vacuum ultraviolet monochromator was employed for these measurements which utilized a 1-meter radius, 600 lines/mm, concave grating blazed at 1500Å. This mounting has fixed

entrance and exit slits at an angular separation of 15 degrees. The grating was over-coated with fresh aluminum and 250Å of MgF_2 to enhance its efficiency down to at least 1000Å. The light source, a windowless d.c. capillary discharge tube, was used to obtain the resonance lines of the rare gases, the Lyman series in hydrogen, and the molecular hydrogen spectrum.

2. Experimental Chamber

A 20" diameter vacuum chamber was attached to the exit arm of the monochromator. This chamber and pumping system could be isolated from the monochromator. All of the measurements were made with a chamber pressure on the order of 5×10^{-5} mm Hg.

The detector was mounted in the experimental chamber on a table which could be rotated from outside the vacuum system. The sample to be studied was mounted in a holder which could be moved vertically in and out of the exit beam and rotated about a vertical axis intersecting the beam. These relationships are indicated in Fig. 1. The sample holder was mounted so that the sample surface was located at the center of rotation of the detector table.

The signal from the detector, a magnetic multiplier with a tungsten photocathode (insensitive above 1600Å) was fed into a d.c. amplifier and recorded.

B. Procedure

Let us assume a beam of intensity I_0 to be incident on a scattering surface, and a detector, of area A, scanning the scattered radiation

at a constant radial separation, r, from that surface. Let θ be the angle of observation relative to the incident beam, and $I_s(\theta)$ the intensity of the scattered radiation observed by the detector at that angle. Then, assuming $I_s(\theta)$ is properly averaged over any directional anisotropies in the scattering distribution, the ratio of the total scattered intensity to the incident intensity is given by:

$$\frac{2\pi r^2}{AIo} \int_0^{\frac{\pi}{2}} I_s(\theta) \sin\theta \, d\theta$$

To obtain a detector having a uniform response, the surface sensitivity of the photo-cathode was mapped using various dynode voltages. The voltages yielding the most uniform response were used and the detector was ultimately masked to a selected 9mm x 9mm area.

The grating was masked to limit the exit beam divergence to 1.5 degrees vertically and 1.5 degrees horizontally. The height of the exit slit was reduced to give a beam 3mm high at the scattering sample. These adjustments resulted in an exit beam cross section of 3mm x 3mm on the sample.

The scattering sample was set normal to the beam and measurements were made every 5° from 10° to 80° on each side of the optical axis. The scattering sample was then set at an angle of 10° and the specular peak was scanned. The sample was then rotated through 90° about an axis perpendicular to its face and the above procedure repeated so as to detect any anisotropies in the scattering distribution.

The intensity of the incident beam was measured by moving the scattering sample vertically out of the beam; however, the direct beam signal was higher than the scatter signal by a factor of 10^2 - 10^5. To reduce the demands on the linearity of the detector, an attenuating screen was used in the measurement of the incident beam. The screen transmission (2.1%) was measured using the same geometry and wavelength as used in the scatter measurement.

C. Results

The samples of gold-black measured in these experiments were prepared by a thermopile manufacturer and are typical of the blacks used on thermopiles for the far ultraviolet. Two thicknesses of black on gold leaf substrates were studied. The thinner of the two blacks, and the black deposited on the thermopile discussed in Sections III and IV of this paper, were manufactured in the same evaporation. This thermopile has a time constant of roughly 0.04 sec. The thicker gold-black, if applied to the same thermopile, would yield a longer time constant - which the manufacturer suggests would be on the order of 0.09 sec.

As a preliminary check of the scatter-measuring apparatus, a sample of silica was studied which had been given a "super-smooth" optical polish*

*This sample was kindly supplied to us by H.E. Bennett. The bowl-feed polishing technique used has been described.[14]

The signal recorded by the detector when scanned through the direct beam is indicated on a semi-log plot in Fig. 2 for radiation of wavelength 584Å. On the same graph the signal recorded when the detector was scanned through the beam reflected from the silica plate is indicated. An angle of incidence of 10° was used. The angular distribution of the reflected beam in Fig. 2 has been normalized to the direct beam distribution at the center. The "tails" of the direct beam distribution are probably due to scattering off the exit slit jaws. The detector signal remains low over the remainder of the scanning range, indicating that light scattered from the measuring chamber walls is negligible. It can be seen that the angular distribution of the reflected beam closely follows the distribution of the direct beam. This indicates that the super-smooth flat does not scatter appreciably at λ584Å, and that the measuring apparatus is not recording unwanted scattered light signals.

Figure 3 indicates the ratio $I_s(\theta)/I_o$ as a function of θ obtained at λ1025Å when the scattering surface was the thinner of the two gold-black samples (presumably identical to that used on the thermopile tested in Sections III and IV). In Fig. 3, two scans are shown - the difference between them being a 90 degree rotation of the scattering sample about the incident beam axis. The difference between the two curves indicates some anisotropy in the angular scattering by the gold-black. Also shown in Fig. 3 is a curve representing the distribution of a "perfect" scattering surface - i.e. where $I_s(\theta)/I_o \sim$ cosine θ. It is apparent

that the angular distribution of the scattering by the gold-black-on-gold resembles the distribution of a perfect scattering surface, with a specular reflection component added on. The specular component is due to the gold substrate which is not completely obscured by the gold-black deposit. The peak of this specular component is less than 0.014% of I_o. The total scattered intensity, obtained from this distribution by the integration indicated in Sec. IIB, is 3.1%. A similar distribution was obtained for this sample of gold-black at λ584Å and at λ1216Å. The integrated scattered radiation at λ584Å was 3.6% and at λ1216Å was 3.1%.

The specular component of the reflectively scattered radiation was absent in the heavier gold-black-on-gold sample tested - as can be seen in Fig. 4 where the distributions are plotted for the same three wavelengths in the far ultraviolet. It can be seen that the scattering loss increases slightly with decreasing wavelength which may reflect the changing ratio of wavelength to particle size of the gold-black. The integrated total scattering for this heavier black was 2.1% at λ584A, 2.0% at λ1025Å was 1.9% at λ1216Å.

These same two samples of gold-black-on-gold were tested for total scattering in the visible and near-infrared spectral regions using an integrating sphere and an appropriate spectrophotometer. The thin sample showed a total scatter of 1.6 - 3.1(±0.5)% and the thicker sample 1.5 - 2.9 (±0.5)% over the region 0.4μ to 2.2μ. Thus, while reflective scattering is a non-negligible loss for thermopile blacks, it would seem that the similarity of this loss in the visible and the far ultra-violet indicates

that the uncertainty in the use of the thermopile at the short wavelengths after calibrating in the visible is less than a percent.

III. Thermopile Cooling due to Ejected Photoelectrons

Two independent methods have been used to determine the loss of thermopile signal due to the cooling caused by the loss of photoejected electrons. In each method, the basic idea is to eliminate the energy loss mechanism due to the photoelectric effect by returning the electrons to the thermopile with the same energy which they carried away. The first method is to surround the thermopile with an electrostatic field sufficiently strong to prevent a loss of photoelectrons. Care must be taken to prevent driving stray electrons and/or negative ions into the thermopile. The second is to emerse the thermopile in a d.c. magnetic field so that ejected electrons will be turned back to the surface. This method has the advantage that stray electrons or ions are repelled from the thermopile.

A. Experimental arrangement

The monochromator and light source described in part II were used for these measurements. However, for this part of the work the radiation from the source was chopped between the source and the monochromator entrance slit with a frequency of 13 ~~cps~~ c/s. The chopping motion, the mechanical design of which has been described,[15] was fed into the vacuum system through a bellows seal. A substantial gain in signal-to-scattered light ratio can be achieved by the proper choice of chopper blade materials. An additional advantage to the use of chopped source radiation applies when

a thermal detector is used; namely, the d.c. voltage generated at the detector due to thermal radiation within the monochromator itself is not accepted by the a.c. amplifier.

1. Thermopile

The thermopile used for this experiment is a series connection of four elements which are composed of bismuth-tellurium and bismuth-antimony alloys.* The thermal junctions are extended using gold flakes of 1mm x 2mm area. Together they form a sensitive area 1mm x 8mm. The thermopile is compensated, designed for a 13 ~~cps~~ c/s chopping frequency and constructed entirely of non-magnetic materials. The thin gold-black coating on the gold flakes is similar, if not identical, to the thin black tested for scattering in Section II. The time constant of the thermopile is on the order of 0.04 sec. and when calibrated in the visible the evacuated thermopile had a sensitivity of 4v/watt and an ENI power of approximately 10^{-9} watts.

The thermopile was located approximately 15mm behind the exit slit of the monochromator. This slit was adjusted to 0.6mm width and 7mm height, assuring that all the flux which passed through the exit slit of the monochromator would be intercepted by the sensitive area of the thermopile. The physical housing of the thermopile is indicated in Fig. 5 It was designed so that a d.c. magnet could be placed outside the vacuum housing but in close proximity with the thermopile, which was centered

*This thermopile was manufactured and mounted in a special housing by the C. Reeder Co., Detroit, Michigan.

between the poles with the magnetic field lines parallel to the long dimension of the sensitive surface.

2. Electronics

An impedance matching transformer was utilized between the thermopile and a pre-amplifier. The thermopile could either be grounded to its surroundings, or made electro-positive with a variety of potentials available from battery sources. (as indicated in Fig. 6.)

A block diagram indicating the overall experimental system is shown in Fig. 7. The signal from the pre-amplifier was fed to a 13 ~~cps~~ c/s broadly-tuned amplifier. The output of this amplifier was rectified synchronously with the chopping frequency by a mechanically coupled rectifier. The signal was then filtered, further amplified and fed into a voltage-to-frequency converter. The converter signal was fed to a 10^5 count scaler. By proper adjustment of the voltage to the converter, the signal could be integrated for any desired period.† In addition to the counter readout, a recorder continuously displayed the rectified and filtered output of the 13 ~~cps~~ c/s amplifier. Thus the source stability during the integration time could be monitored.

Backgound due to local interference was reduced to a negligible level by placing the electronics and the experimental apparatus inside a double Faraday cage.

---

†The use of the voltage-to-frequency converter and scaler system was inspired by a visit to the laboratory of H.E. Bennett who has been using this method for infrared signal detection.

B. Electrostatic Method

1. Procedure

The thermopile signal was first recorded without biasing the element with respect to its surroundings. Then, a d.c. bias was applied as indicated in Fig. 6, and the signal again recorded. A comparison of these signals should indicate the loss caused by the photo-ejected electrons carrying away a portion of the incident radiant energy, assuming the bias voltage was sufficiently high and that no stray electrons or ions were being driven erroneously into the thermopile. Early results indicated some difficulty with the latter effect, probably due primarily to photoelectrons from the exit slit jaws. A positively biased collector electrode was installed on the monochromator side of the exit slit (see "C" in Fig. 5) in an attempt to collect these stray electrons before they were influenced by the retarding field of the thermopile.

The change in thermopile signal resulting from an increase in the collector potential is indicated in Fig. 8, for three thermopile bias potentials, at λ584Å. It can be seen that a collector potential of +45 volts with respect to the grounded monochromator was sufficient to eliminate the effects of the unwanted electrons and ions. Furthermore, it is apparent that a thermopile bias voltage of +45 volts with respect to the grounded surroundings ~~is~~ were sufficient to retard essentially all of the ejected electrons. For the purpose of obtaining the data below, the thermopile retarding potential and the collector ring potential were set at +67 volts.

2. Results

The change in the thermopile signal caused by switching on and off the electrostatic retarding field is shown in Fig. 9 for a number of wavelengths. The data were obtained by allowing the scaler to integrate the signal for 10 seconds without a retarding field, then for 10 seconds with a retarding field. The procedure was continued for 10 or 12 cycles allowing a good check on zero drifts and light source fluxuations.

C. Magnetic Method

The maximum orbital radius of electrons photo-ejected from the thermopile surface in the presence of a magnetic field is readily calculated from the following equation:

$$r = \frac{\sqrt{2mE}}{Be}$$

where m, e are the mass and charge of the electron, E is the electron energy and B the magnetic field strength. For illustration let us consider electrons leaving with 40 eV energy - remembering, however, that most photo-ejected electrons are expected to have energies well below that of the incident photons due to scattering effects in the solid. In the case of 40 eV electrons a magnetic field strength of 1000 gauss yields a maximum orbital radius of 0.2mm.

The maximum radius orbit is achieved when the velocity of the ejected electron is normal to the magnetic field. If the thermopile surface is parallel to the field, and one assumes an electron leaving the surface with a velocity oriented 1° from the direction of the field

of strength 1000 gauss with an energy of 40 eV then the electron will cycloid back to the surface in approximately a 1.3mm vertical displacement. One can conclude from these considerations that a negligible number of photo-ejected electrons would be expected to escape from a 1mm x 8mm thermopile emersed in a 1000 gauss magnetic field for photon energies up to 100 eV. Furthermore, electrons and ions from the monochromator would have little chance of striking the thermopile.

In the present experiment, a permanent magnet with a gap field of 1600 gauss was used. The housing and exit slit (as well as the thermopile) were constructed of non-magnetic materials. The thermopile signal was recorded with and without the magnet positioned as shown in Fig. 5. The data taking procedure was the same as that described for the electrostatic field method in Section III A. The change in the thermopile signal expressed in percent is shown for various wavelengths in Fig. 9, where the data compare favorably with the results of the electrostatic field method. The solid curve shown in Fig. 9 is merely a guide through the experimental points.

The enhancement of the thermopile signal in the presence of the magnetic field was also checked in the visible spectral region as a safeguard against extraneous effects. Application of the magnetic field caused no change in signal when visible light was incident upon the thermopile.

IV. Surface Sensitivity Maps and Time Constant Considerations

If the time constant of the thermopile is not short compared

with the chopping period, a drop in overall a.c. sensitivity will occur. A change of the time constant with wavelength would, in this case, cause variations in a.c. sensitivity such as have been previously noted.[11] A thermopile calibrated in the visible would therefore give erroneous results if used in the far ultraviolet. A d.c. method would circumvent this difficulty, but the a.c. technique has a great advantage in discriminating against unwanted signals.

If the experimental arrangement used for the calibration in the visible is identical to that of the far ultraviolet application, it would seem that a wavelength dependence of the time constant could only be effected by a change in the absorption process - such as a variation in the penetration of the radiation in the absorbing black. Without dwelling on the possible mechanism for such a time constant variation, it is of practical importance to determine the extent to which it exists in a typical far ultraviolet thermopile. In this section we report on measurements which yield a map of the sensitivity variation over the surface of the thermopile, using both visible and far ultraviolet incident radiation, and both a.c. and d.c. methods. Any difference between the a.c. and the d.c. maps would indicate the extent to which the time constant of the thermopile was not negligibly short with respect to the chopping period, and any variation of the a.c. maps with wavelength would be a danger sign in the a.c. use of the thermopile outside the wavelength range of the calibration.

A. Experimental Procedure

The monochromator and light source were described in Section II,

and the thermopile in Section III. For these measurements the thermopile was mounted 8mm from the exit slit on a platform which could be translated perpendicular to the exit beam. The exit beam was limited so that its cross-section at the thermopile was 0.3mm x 8.0mm, with the long dimension vertical. The thermopile was oriented in the beam with its long dimension horizontal - parallel to the translational direction of the table on which it was mounted. The thermopile was then scanned slowly through the beam and a one-dimensional map of the surface sensitivity was determined at different wavelengths.

The output of the thermopile was measured by two methods. In the first, an unchopped light source was used and the thermopile signal was amplified with a d.c. amplifier and displayed on a recorder. In the second, the light source was chopped at 13 ~~cps~~ c/s and the signal amplified using a broad band 13 ~~cps~~ c/s amplifier. The output of the amplifier was rectified synchronously with the chopping frequency, filtered, and displayed on a recorder

B. Results

The one-dimensional sensitivity maps of the thermopile which were obtained at 5461Å, 1606Å and 584Å are shown in Fig. 10. Data obtained by both the a.c. and d.c. methods are indicated. The a.c. and d.c. data obtained at each wavelength are arbitrarily normalized since only the variation in sensitivity along the thermopile is of interest. The curves for three wavelengths have been given an arbitrary vertical displacement in Fig. 10. It can be seen that the a.c. and d.c. sensitivity

maps for each wavelength are essentially identical - the deviations being within the combined reproducibility of these measurements. The curves show, incidentally, that the thermopile deviates considerably from uniform sensitivity along its length. The four segments of the thermopile can be easily recognized, and it is apparent that they are not all equally effective. Furthermore, it is obvious (and expected) that the thermal emf generated at the two ends of each extended junction are not equal in magnitude - thus the sensitivity of each segment is a ramp function. Since the a.c. and d.c. sensitivity maps are essentially identical at all wavelengths studied (several intermediate wavelengths were examined) it would appear that the time constant for this thermopile is, effectively, short compared to the chopping frequency.

In Figure 11 the a.c. sensitivity map for the three wavelengths 5461Å, 1606Å and 584Å are plotted on a single coordinate system. Again an arbitrary normalization has been used. It is apparent from the figure that each of these incident wavelengths produces a nearly identical sensitivity map. From this result we conclude that any variation in the time constant of this thermopile with wavelength is of negligible practical importance.

Sensitivity maps were also obtained with the thermopile rotated through 90° so that its long dimension was parallel to the exit slit. These relatively lower resolution scans produced rather rounded rectangular distribution functions which showed no differences under a.c. and d.c. operation and no wavelength dependence.

V. Conclusions

The foregoing sections have discussed three aspects of the performance of a thermopile which are of importance for radiometric applications in the far ultraviolet. It has been shown that the reflective scattering from thin gold-black-on-gold foil, while not insignificant, is similar in the visible and far ultraviolet. Therefore, if the thermopile is calibrated in the visible and used in the far ultraviolet, this phenomena should not require a correction - if radiometric accuracy in the 1% range is sufficient. It was further determined that this thermopile has a surface sensitivity and a time constant which is independent of wavelength in the regions of interest. It would appear, in fact, that the only significant correction which would be required for this thermopile is due to the photoelectric effect, which causes a negligible loss in the visible region, but as high as a 5% loss in the far ultraviolet.

These results apply only to the thermopile which was used in this study and a generalization of them is not necessarily justified. However, these results increase our confidence in the validity of this method of radiometry for the far ultraviolet. We feel that if these corrections are carefully established for an optimum thermopile, a radiometric detector standard will have been developed for the far ultraviolet which will be reliable in the few percent range, ~~this would be very desirable at the present time~~. If this detector compared favorably with the rare gas ionization chamber detectors[16] in their regions of effectiveness, and with the source standards being developed at NBS[17] in the region above 2000Å, we feel it would be justifiable to use such a thermopile to calibrate more sensitive detectors throughout the far ultraviolet.

References

1) N. Wainfan, W.C. Walker and G.L. Weissler, J. Appl. Phys. 24, 1318 (1953)

2) K. Watanabe, F.F. Marmo and E.C.Y. Inn, Phys. Rev. 91, 1155 (1953)

3) N. Wainfan, E.C. Walker and G.L. Weissler, Phys. Rev. 99, 542 (1955)

4) C. Kenty, Phys. Rev. 44, 891 (1933)

5) R. Baker, J. Opt. Soc. Am. 28, 55 (1938)

6) H.E. Hinteregger and K. Watanabe, J. Opt. Soc. Am. 43, 604 (1953)

7) W.C. Walker, N. Wainfan, G.L. Weissler, J. Appl. Phys. 26, 1366 (1955)

8) D.M. Packer and C. Lock, J. Opt. Soc. Am. 41, 699 (1951)

9) F.S. Johnson, K. Watanabe, R. Tousey, J. Opt. Soc. Am. 41, 702 (1951)

10) K. Watanabe and E.C.Y. Inn, J. Opt. Soc. Am. 43, 32 (1953)

11) R. Stair, W. Schneider, W. Waters, J. Jackson, J. Appl. Optics (In ~~paint~~)

12) A. Smith, Thesis, University of Rochester, 1961

13) L.R. Canfield, private communication

14) W.F. Koehler, J. Opt. Soc. Am, 743 (1953)

15) R.P. Madden and L.R. Canfield, J. Opt. Soc. Am. 51, 838 (1961)

16) J.A.R. Samson, J. Opt. Soc. Am. 54, 6 (1964)

17) H.J. Kostkowski, D.E. Erminy, A.T. Hattenberg, J. Opt. Soc. Am. 54 1386A (1964A)

Figure Captions

1) Diagram showing the experimental arrangement used for the measurement of the reflective scattering from gold-black in the far ultraviolet spectral region. The dashed portion of the diagram indicates the position of the sample and detector when the direct beam is measured.

2) Angular profile of the beam reflectively scattered from a highly polished silica reflector, compared with the profile of the incident beam at $\lambda 584\mathring{A}$. The reflected beam profile is arbitrarily normalized to the incident beam profile at the maximum (angle of incidence = 10°)

3) Angular profile of the beam reflectively scattered from a sample of gold-black on a gold substrate. The ordinate is the ratio of the scattered intensity at angle θ to the incident beam intensity. A cosine distribution (perfect scatterer) is shown for comparison. Note the specular peak which is apparent for this thickness of black. When used on a thermopile, this thickness resulted in an overall time constant of 0.04 sec. ($\lambda = 1025\mathring{A}$)

4) Angular profile of the beam reflectively scattered from a second sample of gold-black (thicker than that used for Fig. 3) on a gold substrate at three wavelength in the far ultraviolet. The ordinate is the ratio of the scattered intensity at angle θ to the incident beam intensity.

5) A sectional drawing of the exit slit and thermopile housing, showing the relative locations of the exit slit (S) and thermopile (T). The collector ring (C) is used in the electrostatic method of returning photo-ejected electrons to the thermopile: The magnet (M) is used in the magnetic method.

6) Circuit diagram showing the method used to bias the thermopile electropositive with respect to its surroundings.

7) Block diagram of the overall experimental arrangement indicating, in particular, the detection scheme which has proven effective in obtaining accurate results with the low signal-to-noise usually associated with thermopile detection.

8) Thermopile response vs. collector potential for several thermopile bias voltage. The bias voltage (See Fig. 6) provides the electrostatic field to return photo-ejected electrons to the thermopile. The collector ring potential (See Fig. 5) is required to prevent stray electrons or ions from reaching the thermopile

9) The percent increase in thermopile signal achieved by returning the photo-ejected electrons to the detector, as a function of wavelength in the far ultraviolet. The results of the electrostatic method and the magnetic method are compared. The solid line merely connects the experimental points.

10) One-dimensional sensitivity maps showing the variation of the thermopile response as a function of displacement along the long dimension of the thermopile. The data obtained at three wavelengths

are shown, and the results using d.c. detection are compared with those using a.c. synchronous detection and 13 ~~cps~~ c/s chopping. The data obtained at the three wavelengths (A - 584Å; B - 1606Å; C - 5461Å) have been given arbitrary vertical displacements. The results of the a.c. method are arbitrarily normalized to the results of the d.c. method for each wavelength.

11) One-dimensional sensitivity maps showing the variation of the thermopile response as a function of displacement along the long dimension of the thermopile for three different wavelengths. Only the results from the a.c. detection method (13 ~~cps~~ c/s chopping) are shown. The scans for the different wavelengths were arbitrarily normalized at one point along the thermopile.

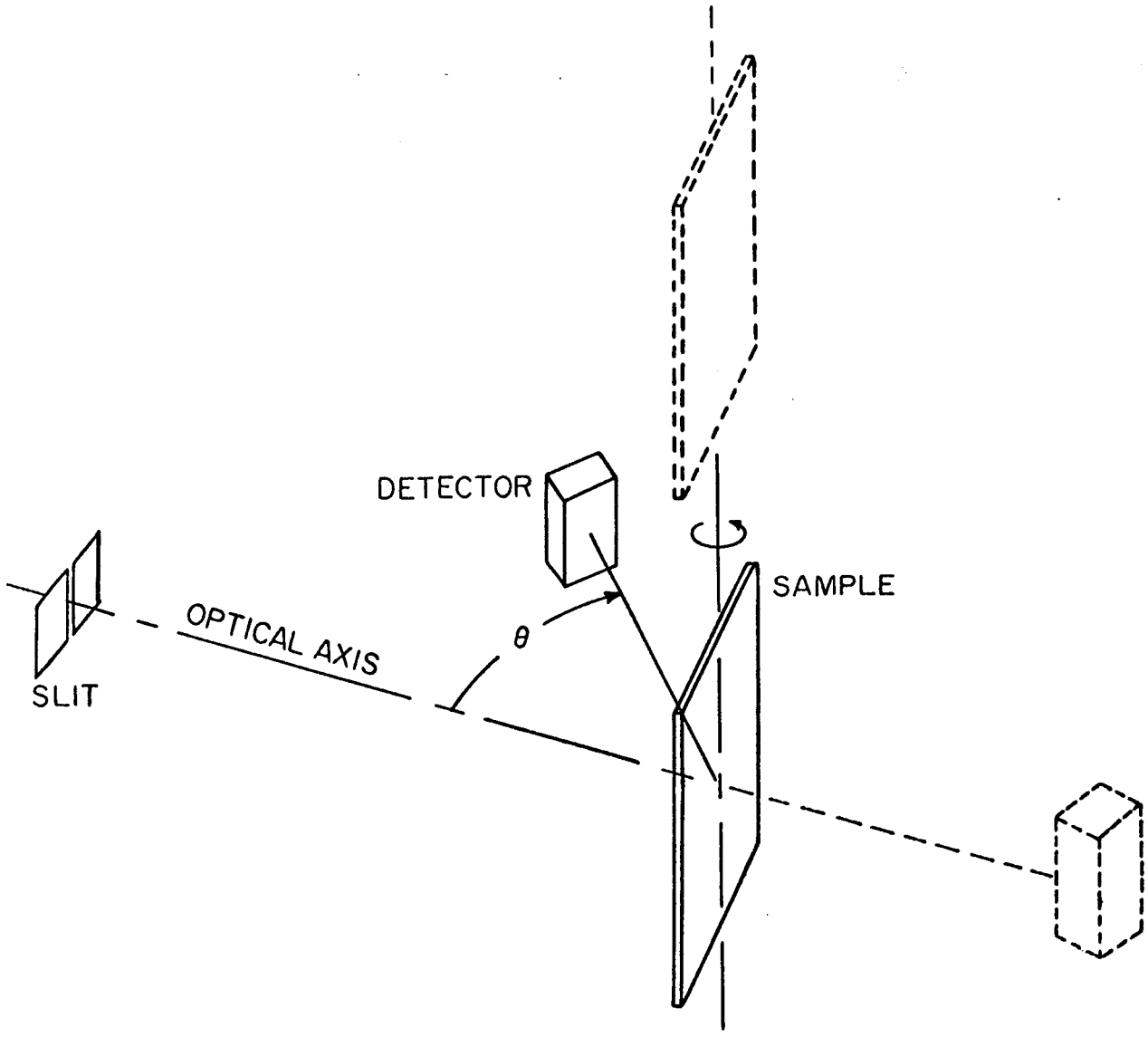
DETECTOR
SAMPLE
OPTICAL AXIS
θ
SLIT

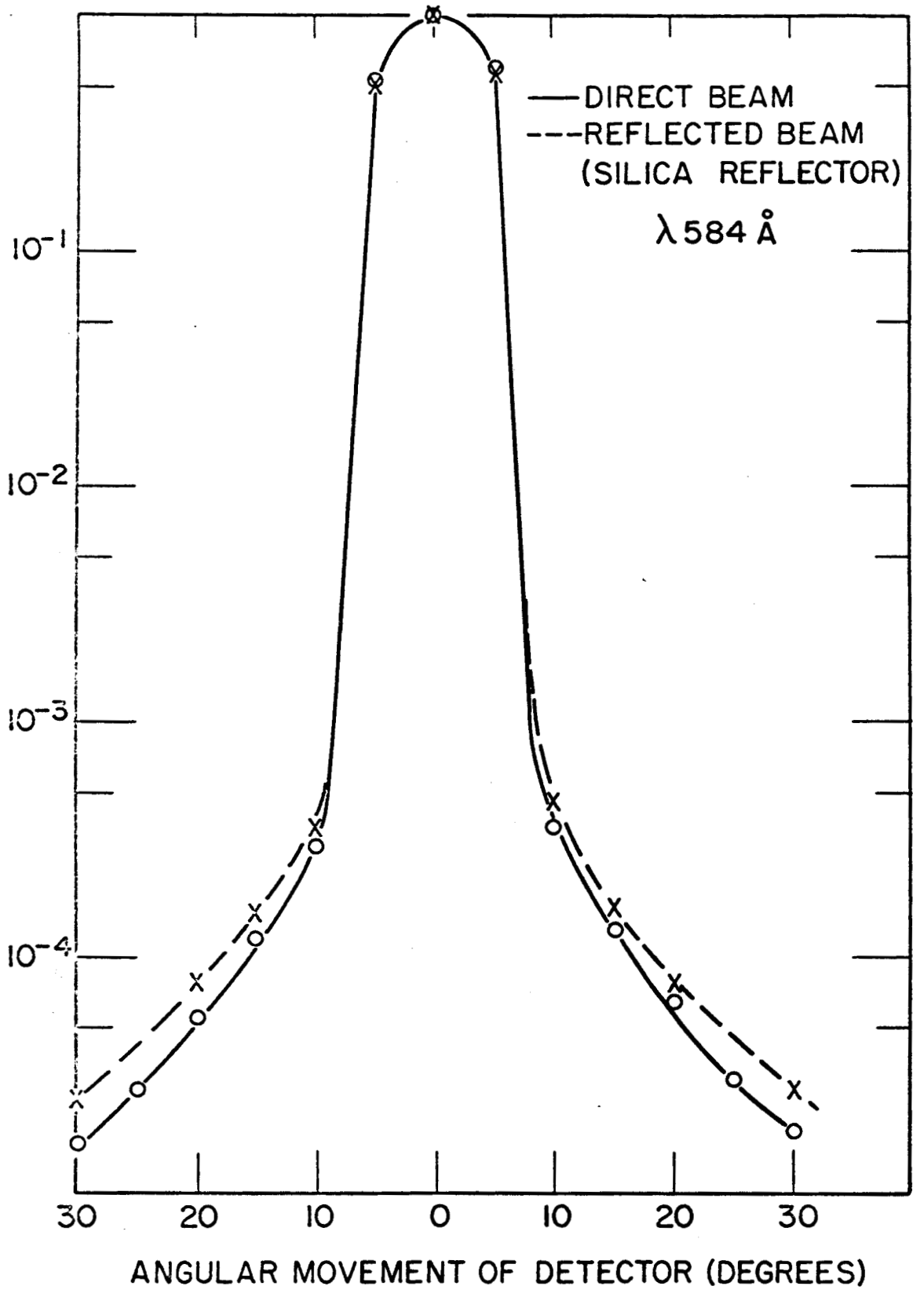
DIRECT BEAM
REFLECTED BEAM
(SILICA REFLECTOR)
λ 584 Å
10⁻¹
10⁻²
10⁻³
10⁻⁴
30
20
10
0
10
20
30
ANGULAR MOVEMENT OF DETECTOR (DEGREES)

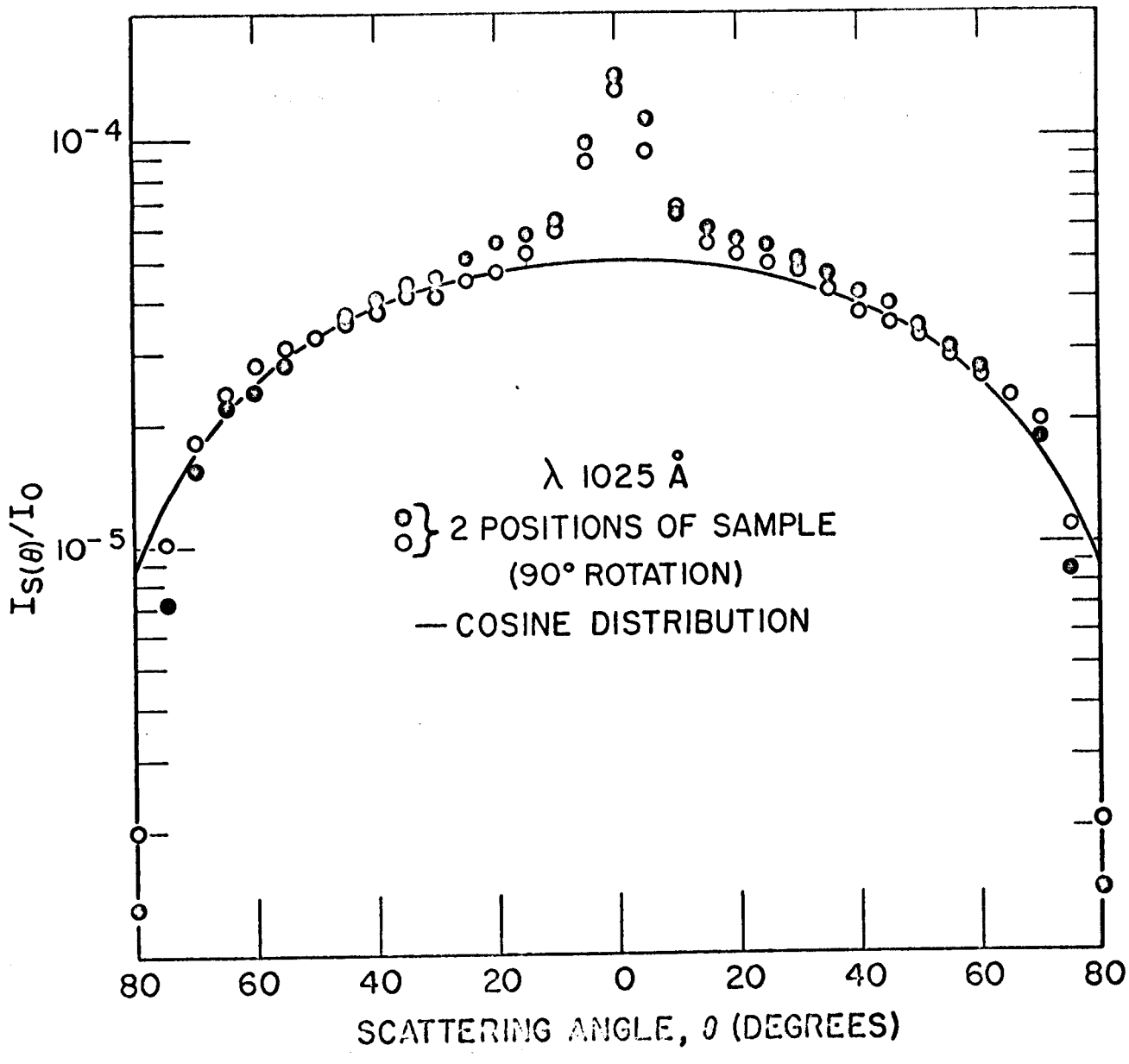
10^{-4}
10^{-5}
$I_{S(\theta)}/I_0$
λ 1025 Å
2 POSITIONS OF SAMPLE
(90° ROTATION)
— COSINE DISTRIBUTION
80
60
40
20
0
20
40
60
80
SCATTERING ANGLE, θ (DEGREES)

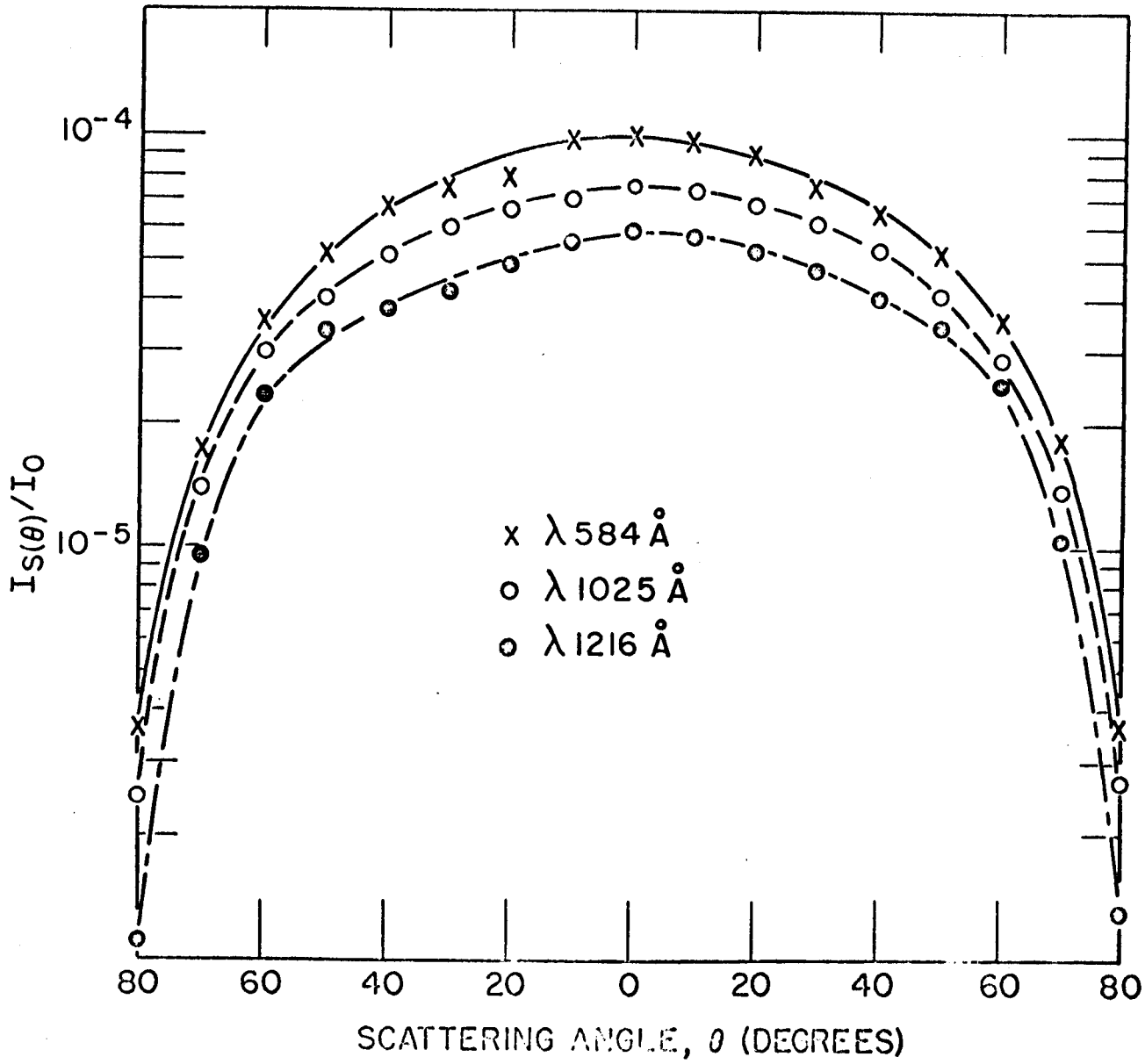
10^{-4}
10^{-5}
$I_{S(\theta)}/I_0$
x λ584 Å
o λ1025 Å
o λ1216 Å
80
60
40
20
0
20
40
60
80
SCATTERING ANGLE, θ (DEGREES)

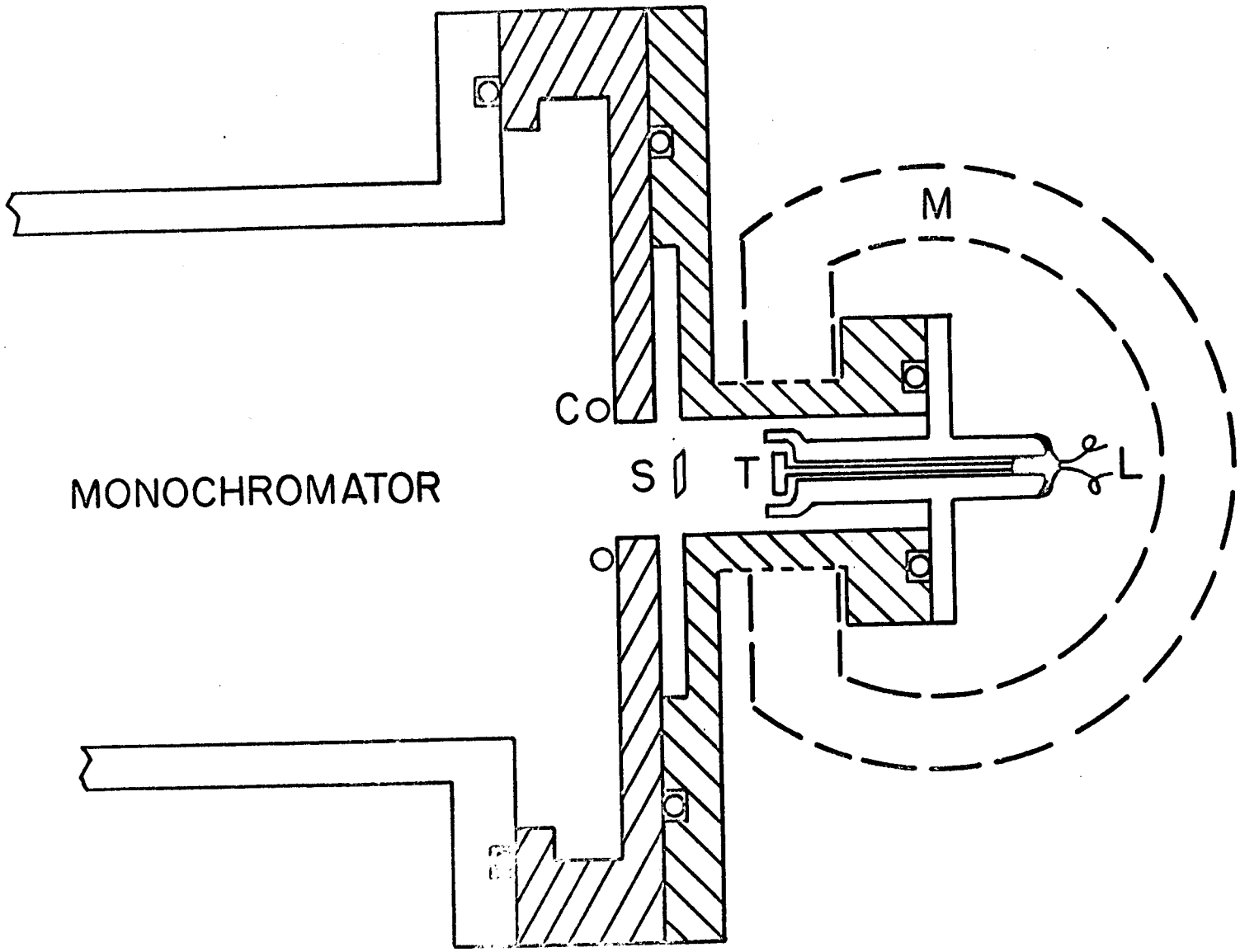
M
C
S
T
L
MONOCHROMATOR

TO
PREAMPLIFIER
SHIELD
THERMOPILE

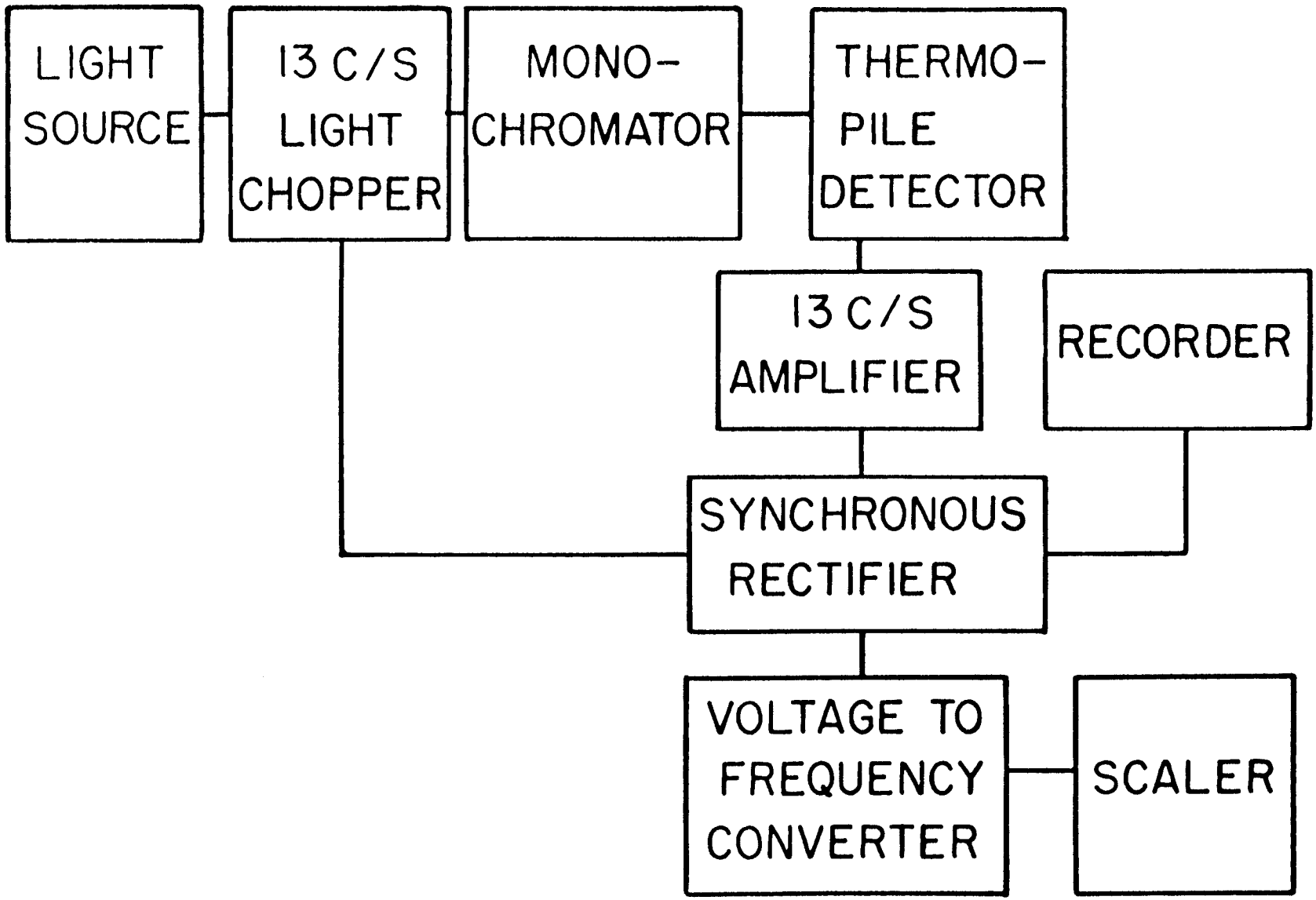
LIGHT SOURCE
13 C/S LIGHT CHOPPER
MONO-CHROMATOR
THERMO-PILE DETECTOR
13 C/S AMPLIFIER
RECORDER
SYNCHRONOUS RECTIFIER
VOLTAGE TO FREQUENCY CONVERTER
SCALER

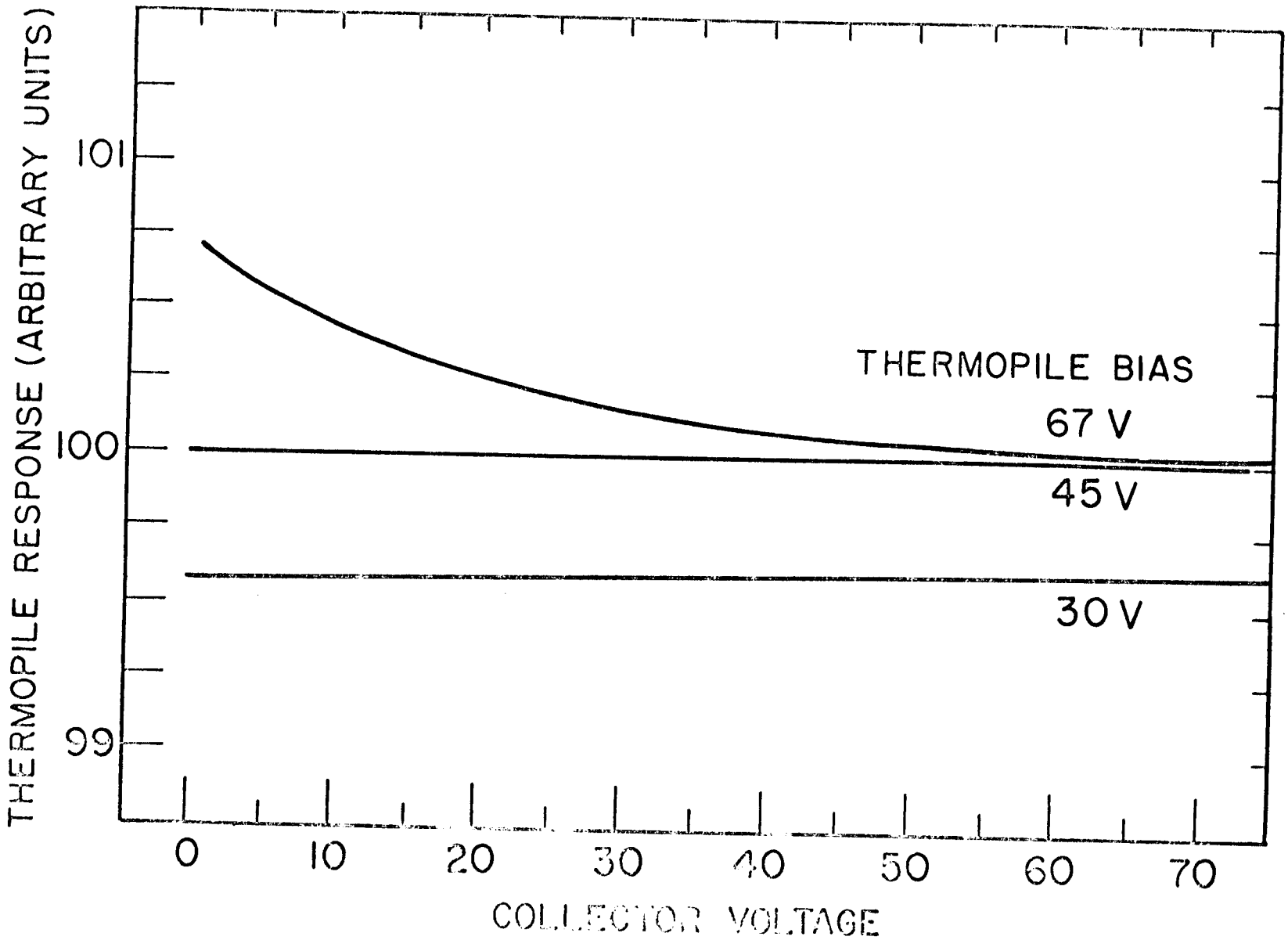
THERMOPILE RESPONSE (ARBITRARY UNITS)
101
100
99
THERMOPILE BIAS
67 V
45 V
30 V
0
10
20
30
40
50
60
70
COLLECTOR VOLTAGE

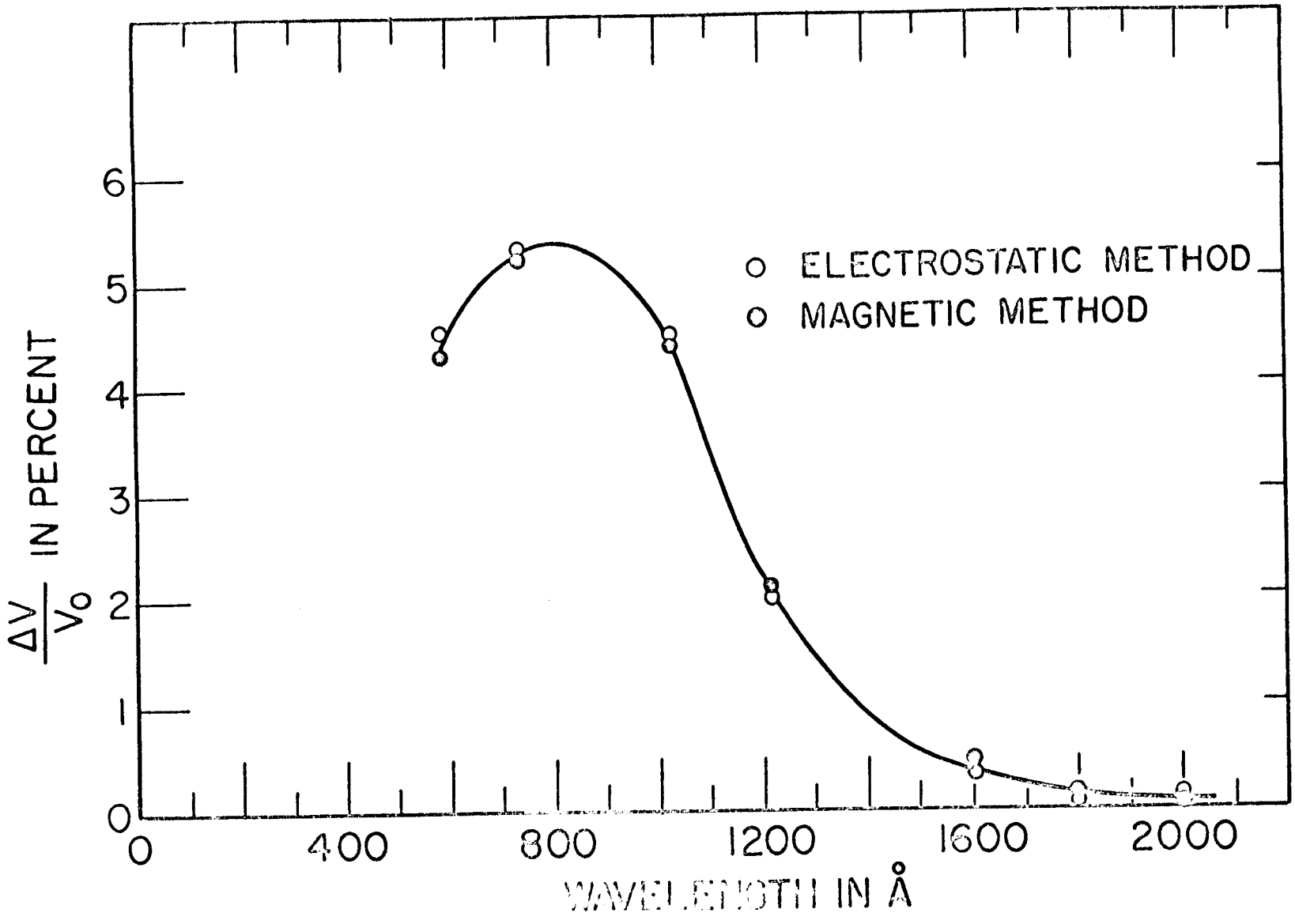
ELECTROSTATIC METHOD
MAGNETIC METHOD
$\frac{\Delta V}{V_0}$ IN PERCENT
0
1
2
3
4
5
6
0
400
800
1200
1600
2000
WAVELENGTH IN Å

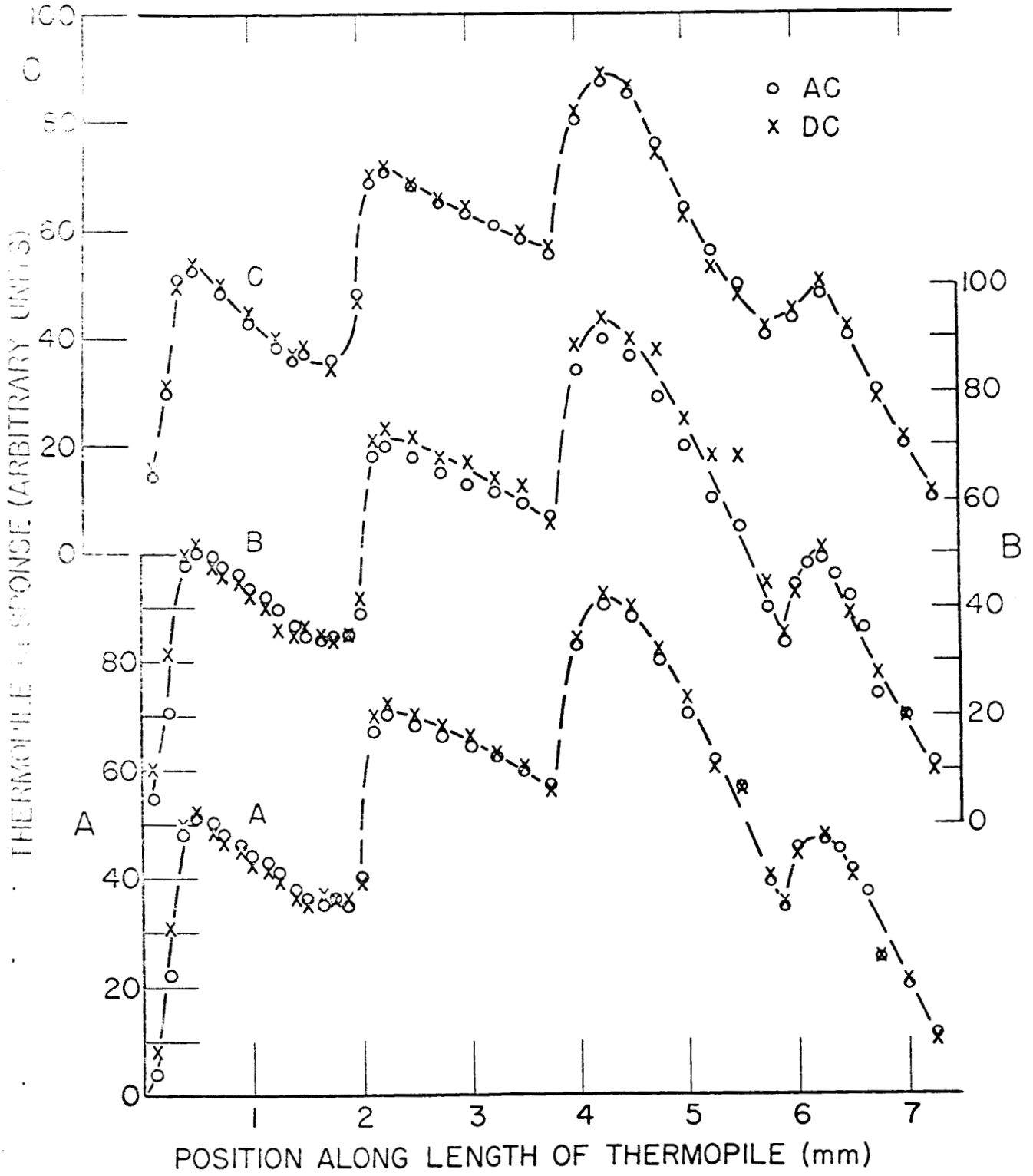
AC
DC
C
B
A
THERMOPILE RESPONSE (ARBITRARY UNITS)
POSITION ALONG LENGTH OF THERMOPILE (mm)
0
20
40
60
80
100
1
2
3
4
5
6
7

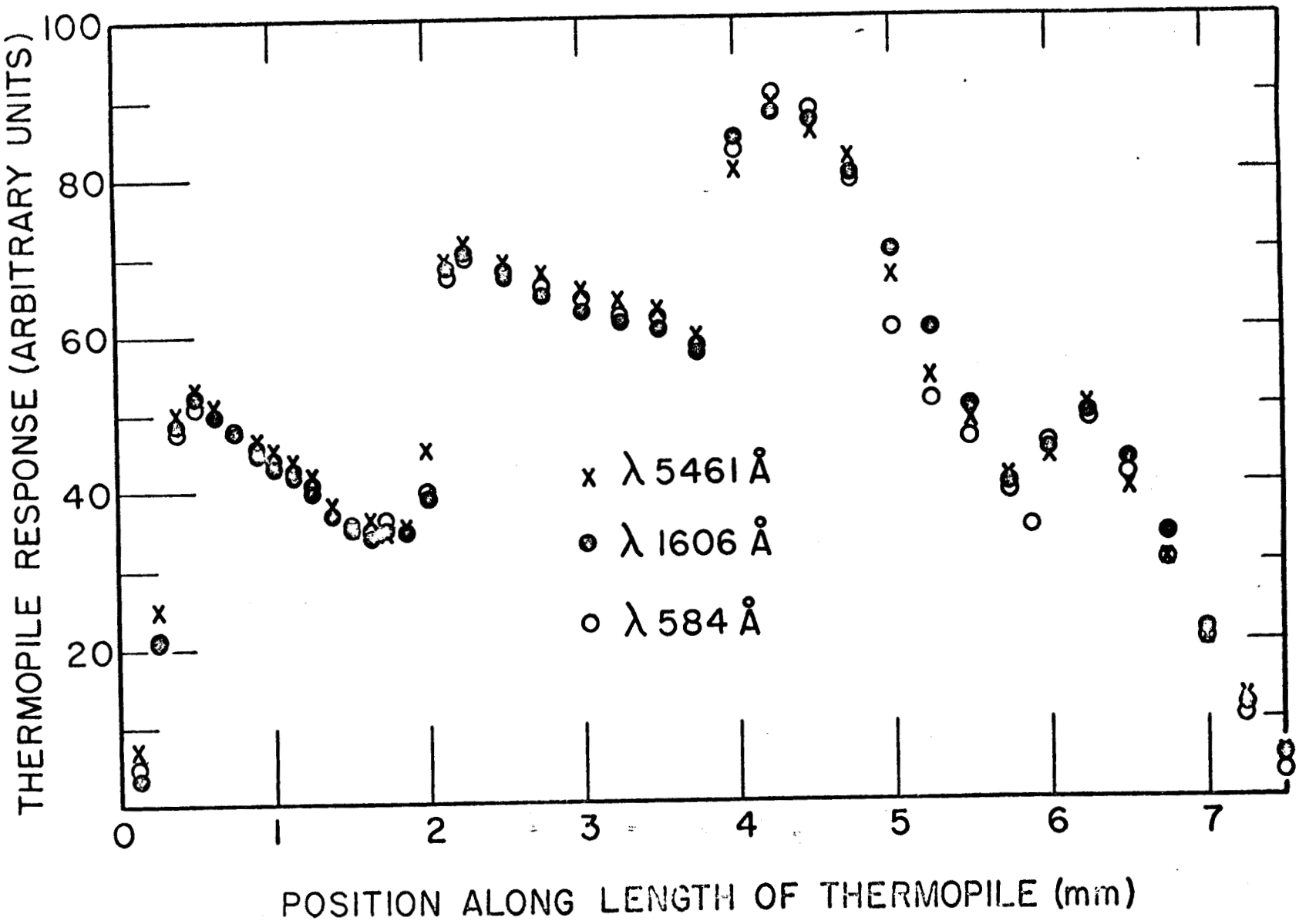
THERMOPILE RESPONSE (ARBITRARY UNITS)
100
80
60
40
20
0
1
2
3
4
5
6
7
POSITION ALONG LENGTH OF THERMOPILE (mm)
x λ 5461 Å
λ 1606 Å
o λ 584 Å